ORIGINAL PAPER

Liquid hydrogen storage design trades for a short-range aircraft concept

Tim Burschyk[1] · Yannic Cabac[1] · Daniel Silberhorn[1] · Brigitte Boden[1] · Björn Nagel[1]

Abstract

Preliminary design trades for the liquid hydrogen storage system of a short-range aircraft are presented. Two promising insulation methods, namely rigid foam and multilayer insulation, are identified as main design drivers. In addition, the maximal pressure and the shape of the hydrogen storage tank influence the aircraft performance and the insulation efficiency. In this study, the hydrogen storage tanks are integrated in wing pods. The main effects driven by the design parameters are addressed using conceptual and preliminary methods: models are carried out for the storage mass, additional drag, propeller efficiency loss and the dynamical thermodynamic behavior of the liquid hydrogen storage. These effects are coupled making an integrated design method necessary. For the sizing of the liquid hydrogen storage, a multidisciplinary workflow is set up including the aircraft sensitivities on the design mission block fuel. The trade-off study reveals the opposing trend between insulation efficiency and aircraft performance. For the insulation architecture based on rigid foam, the penalties implied by the storage tank on aircraft level and the penalties due to vented hydrogen can be balanced and result in minimal block fuel for the design mission. The application of multilayer insulation avoids venting during the design mission, but has an increased penalty on the aircraft performance compared to rigid foam insulation. Besides the criterion of minimal block fuel, the dormancy time is compared, indicating the thermal efficiency. Applying multilayer insulation, the dormancy time can be increased significantly calling for a discussion of operational requirements for hydrogen-powered aircraft.

Keywords Liquid hydrogen storage design · Trade-off study · Hydrogen-fueled aircraft · Liquid hydrogen storage integration

1 Introduction

Regarding the environmental goals of the aviation industry [1], the application of liquid hydrogen (LH2) as an energy carrier is an ongoing debate. Despite many challenges related with this technology, the integration of the liquid hydrogen storage is seen as one of the main issues: the volume and weight of the storage compartment as well as the cryogenic properties of liquid hydrogen have a significant influence on the aircraft design and performance. Therefore, new aircraft concepts are investigated recently. Several types of LH2 storage integration are discussed in the literature [2–6], each of them coming with specific advantages. The goal of this study is to assess the integration of the storage compartment in wing pods. Wing pods are easy to access and due to its proximity to the consumers, the uncertainties involved with the fuel delivery system design are minimized. On the other hand, the increase of aerodynamic drag implies a drawback to this type of integration compared to, e.g., an integration of the storage tank in the rear [3]. Besides the type of integration, design specifications concerning the liquid hydrogen storage affect the aircraft performance. Therefore, this trade-off study is conducted to provide design trends and to capture the relevant effects and sensitives. The

✉ Tim Burschyk
  tim.burschyk@dlr.de

  Yannic Cabac
  yannic.cabac@dlr.de

  Daniel Silberhorn
  daniel.silberhorn@dlr.de

  Brigitte Boden
  brigitte.boden@dlr.de

  Björn Nagel
  bjoern.nagel@dlr.de

1   Institute of System Architectures in Aeronautics, German
    Aerospace Center, Hein-Saß-Weg 22, 21129 Hamburg,
    Germany

paper is divided into the following parts. Section 2 deals with the methodology and the modeling of the liquid hydrogen storage and its effects on the aircraft performance for this type of integration. In Sect. 3, the conducted parameter study is explained and their results are discussed. Section 4 concludes the paper.

2 Methodology

For the integration of cryogenic hydrogen in an aircraft, many aspects have to be considered. For instance, the aircraft performance is penalized directly by the additional mass of the storage tank and the increase of aerodynamic drag compared to a conventional design. Moreover, the pods interfere with the propeller air flow decreasing the propulsive efficiency. Besides the geometrical and structural integration, the usage of liquid hydrogen implies additional challenges to the design. Due to its cryogenic properties, liquid hydrogen is subject of complex heat and mass transport, resulting in evaporation at steady state and thermal equilibrium. Therefore, vapor must be vented for a given pressure level, which may cause fuel loss depending on the system architecture of the fuel system. Within this study, vented hydrogen is regarded as fuel loss. The intensity of these effects depends on certain design decisions. In this case, the insulation concepts have an impact on the storage mass and the insulation efficiency: a well-insulated storage correlates with a heavy tank. Moreover, the allowable pressure level in combination with the initial fuel condition affects the dormancy time. A subcooled liquid extends the timespan for which venting is not necessary. However, supplying subcooled liquid hydrogen is an energy-intensive process and the trade-off between aircraft performance improvements and ground operations is beyond the scope of this study. Another key design decision is the geometric realization of
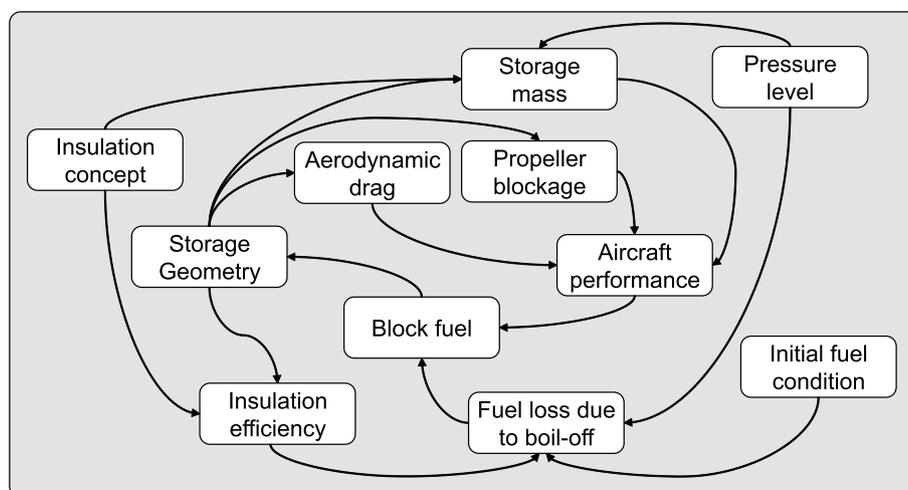
the storage compartment, since the volume-to-surface ratio is an important parameter for the insulation efficiency and the shape affects the aircraft performance directly. Most of the effects depend on each other forming a coupled system. The interaction of these effects is shown qualitatively in Fig. 1. Analyzing the interactions, two feedback loops can be found. The first feedback loop deals with the aircraft performance: the aircraft performance determines the block fuel for the given flight mission. A certain storage volume is needed to store the total amount of fuel. This volume is converted to a shape following external geometry generation rules. Since the shape influences the drag, propeller blockage and storage mass, the first feedback loop is closed. The second feedback loop takes the thermodynamic behavior of the liquid hydrogen storage into account. In case of venting, additional fuel for the mission has to be stored in advance. That changes the amount of the total fuel and influences the storage volume and geometry, respectively. Again, the storage shape is fed back to the insulation efficiency determining the possible fuel loss in case of venting.

Considering the main interdependencies, an integrated design method is required to conduct this trade-off study. The following sections describe the aircraft concept, the modeling of the main effects and the design philosophy.

2.1 Aircraft concept

To study the influence of the LH2 storage integration on aircraft level, a conceptual aircraft design from the German Aerospace Center (DLR) internal project EXACT (Exploration of Electric Aircraft Concepts and Technologies) is used [7]. The design represents an advanced (entry into service in 2040) turboprop aircraft which uses two liquid hydrogen-driven gas turbines for power generation, shown in Fig. 2. Two power trains, each including a gas turbine and a liquid hydrogen storage, are installed into wing pods on each side
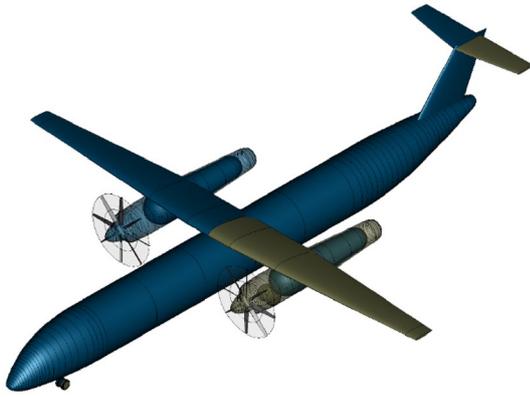

Fig. 1 Complex interaction requires a coupled approach

Fig. 2 LH2-fueled aircraft concept

Table 1 Key aircraft concept characteristics

Parameter	Unit	Value
Entry into service	–	2040
MTOM	t	69.6
OEM	t	43.2
L/D	–	17
Design range	nm	1500
Design payload	t	23.75
Design PAX number	–	250
Design cruise mach number	–	0.62
Initial cruise altitude	ft	27000
Service ceiling	ft	33000

of the wing. Two large propellers mounted in front of the wing pods are used for propulsion.

The overall aircraft design process is supported by various disciplinary tools being integrated into a workflow within the remote component environment (RCE) [8]. The tool openAD [9] is used to initialize the aircraft sizing with a minimal set of top-level aircraft requirements (TLARs) and synthesize the results from the disciplinary tools. This conceptual aircraft design tool is mainly based on empirical and semi-empirical methods and allows a flexible integration of different disciplines within the workflow. Moreover, the flight performance and consumed energy for a specific mission are provided by a DLR-developed trajectory calculation model. Depending on the aerodynamic and engine performance, the equation of motion is solved resulting in a stepwise two-dimensional description of the mission trajectory for the high-speed regime. For the low-speed performance, the tool LSperfo [10] provides the data for take-off and landing. Prior to the design of the LH2-fueled concept aircraft, the workflow has been calibrated with reference data from the A321neo. To enhance the integration of disciplinary tools, the standardized common parametric aircraft configuration schema (CPACS) [11] is used for data exchange.

2.1.1 Key characteristics

The key aircraft characteristics are listed in Table 1. The aircraft is capable of 250 passengers (PAX) in a single class layout and represents a stretched version of a family concept which could be a potential successor of the A320 family. The design range of 1500 nm and Mach number of 0.62 are set in the context of a sustainable short-range turboprop aircraft. The resulting key parameters are, e.g., maximum take-off mass (MTOM) of 69.6 t and lift-to-drag ratio (L/D) of 17. More information on the conceptual aircraft can be obtained from [7].

2.1.2 Block fuel characteristics

To assess the implications of the design choices on the aircraft performance, the sensitivities regarding the block fuel of the design mission are used. The variation of operating empty mass (OEM), zero-lift drag and propulsive efficiency imitates the variation of storage mass, aerodynamic drag and the propeller blockage of the wing pods. To quantify these effects, the aircraft sizing workflow is used, which is explained in Sect. 2.1. To derive the sensitivities, the TLARs are kept fixed for each aircraft sizing loop. Depending on the combined variation of OEM, zero-lift drag and propulsive efficiency, each solution represents a converged aircraft design including resizing effects. For the converged aircraft concepts, the mission performance is calculated and serves as a response surface.

Figure 3 shows exemplary the sensitivities in percent block fuel difference at a propulsive efficiency loss of 1 %
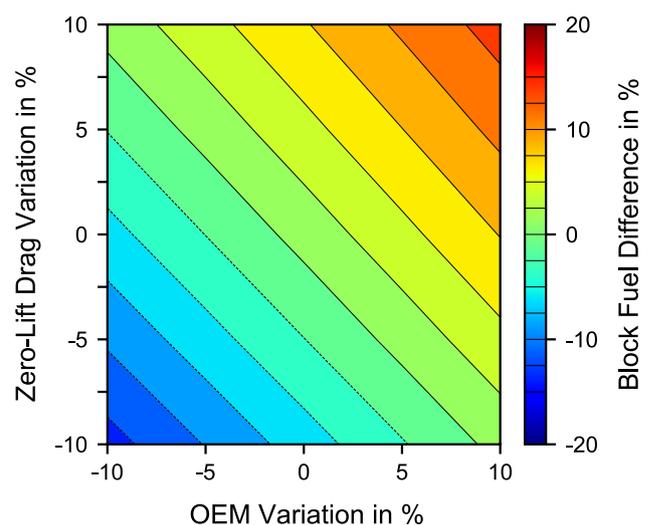

Fig. 3 Aircraft sensitivities in percent block fuel for the design mission at 1 % propulsive efficiency loss

by the variation of zero-lift drag and OEM. The figure indicates a linear dependence of the block fuel difference within the boundaries of the variable parameters.

Assumptions regarding the hydrogen storage tank of the aircraft concept have been made in previous studies. These assumptions serve as a starting point for the evaluation of the penalties implied by the storage tank design within the parameter study. For the storage, mass per tank 1187.5 kg is assumed and the aerodynamic drag per wing pod is set to 1679.1 N. The propulsive efficiency loss due to propeller blockage is presumed to be 1 %. Applying these assumptions for the aircraft concept, the total design mission block fuel is calculated as 2139.4 kg and the design mission fuel reserves to 599.5 kg hydrogen, respectively.

2.2 Storage models

The main effects of the integration approach are considered using conceptional and preliminary design methods at this stage of the study. The following subsections deal with the modeling approaches.

2.2.1 Storage geometry

The shape of the storage geometry can be divided into the following parts: a tank dome, a cylindrical segment and a conical segment closed by a spherical dome. For the front dome, a torispherical configuration is chosen as described in Brewer [4]. The shape of the conical end depends on the maximal diameter: to decrease pressure-induced drag, the ratio of diameter to aft length and aft diameter is kept constant which will be discussed in Sect. 2.2.3. Figure 4 illustrates the variation of the storage geometry for a constant volume and a variable diameter of the cylindrical section. The geometric model for the storage is created using the knowledge-based engineering framework Codex [12]. Using this framework, a parameterized model is generated describing all the layers of the tank. Based on this model,
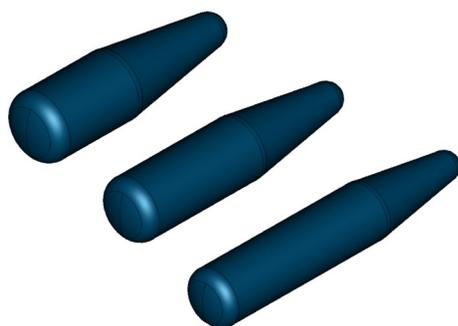
a geometric representation of the tank can be exported and calculations on this geometry can be performed. For example, the fill level and the corresponding interface area between the liquid and gaseous hydrogen can be determined for a given filling ratio. In addition, the volume and surface area of each storage layer are calculated.

2.2.2 Storage mass

The storage mass consists of the storage compartment walls, the insulation layers, adjacent systems and installation penalties. First, the insulation architectures are described followed by the calculation procedure for internal and external overpressure to size the compartment walls. Two insulation architectures are compared within this study. Both of them are displayed in Fig. 5. The first storage concept features a single-wall compartment of aluminum followed by rigid foam, a vapor barrier, soft foam and finally a thin layer of Kevlar. For both concepts, an integral tank design has been chosen for the podded tanks so the last layer is directly exposed to the ambient. This concept is one of the candidate insulation concepts proposed in Brewer [4]. The second insulation architecture is based on a double-walled storage compartment with the space in between evacuated, similar to Stroman et al. [13]. Nevertheless, this insulation inherits some features of the first insulation concept. The outer layers are composed of soft foam and Kevlar and the inner insulation layer consists of rigid foam. This layer is added for safety in case of vacuum loss, as proposed in Brewer [4]. The mass of the operational systems are given by Brewer [4]. Depending on the insulation architecture, a vacuum pump system and a purge system, as well as a pressurization and vent system are needed. In addition, an installation factor referred to the storage mass of about 8 % is applied, which is comparable to the assumed value in Brewer [4]. The mass of the fuel system is included in the aircraft concept.

The storage walls with internal overpressure are sized in accordance with the guidelines of AD2000 [14]. Equation 1
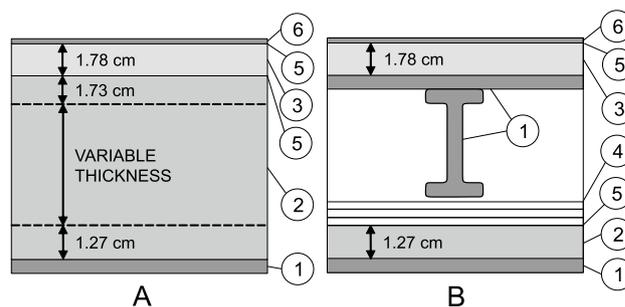

Fig. 4 Iso view on storage geometry; volume is kept constant while the diameter is varied

Fig. 5 Insulation architecture based on the rigid foam (**A**) and multi-layer insulation (**B**). Materials: (1) aluminum, (2) rigid foam, (3) soft foam, (4) multilayer insulation, (5) vapor barrier, (6) Kevlar

shows the minimum required wall thickness t for cylindrical pressure vessels in its original form (additional factors and margins for welding, wear, etc. can be neglected according to the guidelines).

$$t = \frac{D \cdot p}{2\sigma/S + p} \tag{1}$$

The pressure p usually represents the limit pressure defined as the maximum pressure that is allowed during operation. Instead of the limit pressure, an ultimate pressure is used to account for additional loads from gusts and maneuvers. According to Brewer [4], the ultimate pressure equals 1.5 times the limit pressure. The stress σ depends on the material's resistance. According to Brewer's fatigue analysis, a design stress of 172 MPa can be used for aluminum alloy 2219 T851 considering a maximum of 40,000 cycles [4]. The safety factor S is set to 1.5 which is usually used in aviation. For the dome and cone section, the same wall thickness is assumed as required in the cylindrical section. This assumption allows for a simplified geometry generation reducing the complexity of the thermodynamic modeling. A dome- and cone-specific wall thickness determination approach from the AD2000 [14] showed a neglectable wall increase compared to the cylindrical approach for torispherical domes and cone angles below 10°, respectively. For the double-walled storage structure, a hard vacuum is applied to fulfill the requirements of the multilayer insulation. Therefore, the outer aluminum vessel has to be sized for external overpressure. The calculation of the wall thickness is conducted following the calculation procedure suggested in [14] for cylindrical pressure vessels exposed to external overpressure. Plastic deformation and elastic instability are the sizing parameters according to [14]. For the material properties, the same assumptions are made as for the internal overpressure. An ovality of 1.5 % is allowed. To minimize the wall thickness, a stiffener concept is applied as proposed by the calculation procedure. Therefore, double-T beams with a length of 50 mm and outer width of 10 mm serve as stiffeners. The unsupported length between the stiffeners is optimized to ensure a lightweight combination of wall thickness and stiffener distance. The mass is calculated as mass per area including stiffener mass and mass of the wall. This is applied to the surface area of the MLI layer.

2.2.3 Aerodynamic drag

The aerodynamic drag is assessed according to Torenbeek [15]. The proposed method accounts for the profile drag of cylindrical bodies including variable nose and tail sections, such as fuselages and wing pods. Torenbeek's method is not only well suited for the present drag estimation as it represents a simple approach on the one hand, but it is also

sensitive for a variation of the nose and tail geometry on the other hand. Equation 2 shows the composition of the profile or base drag coefficient $D_{D,b}$.

$$D_{D,b} = D_{f,2D} \cdot (1 + f_s) + \Delta D_{D,p} \tag{2}$$

The flat plate friction drag coefficient $D_{f,2D}$ is determined by an empiric correlation for turbulent flow according to Schlichting and Truckenbrodt [16] (assuming turbulent flow along the whole length). Pressure drag is considered by the shape factor f_s. The drag increment $\Delta D_{D,p}$ accounts for the additional pressure drag of short-tail sections (tail length smaller than two times the diameter). For more details concerning the parameter determination and a detailed description of the drag coefficient estimation in Eq. 2 the reader is refered to [15]. The aerodynamic relevant shape, being exposed to the free stream, and thus the overall wetted surface includes the outer storage surface itself (except for the pressure dome) and an additional covered installation space in front of it. The resulting intersected body, here referred to as the wing pod fairing, is shown in Fig. 6.

The fairing's nose and tail section length can be optimized in terms of minimizing the overall fairing drag while providing sufficient space for fuel and systems. For the nose section, the optimum length is found to equal its base radius. For the tail section, the optimum length is found to be equal to two times its base diameter. For the following drag penalty assessment, cruise conditions are assumed. In addition, two installation factors are applied: 1.1 for interference drag and 1.05 for additional friction drag due to the slipstream of the propeller.

2.2.4 Propeller blockage

Propeller blockage refers to the effect of retarding the airflow through the propeller caused by an object (e.g., fuselage, nacelle or wing pod) directly behind it [17]. The blockage effect is considered by reducing the propeller efficiency compared to an isolated propeller. A conservative approach is chosen as the propeller is designed for variable 'fictive' spinner radius representing the presence of the pod fairing downstream. Consequently, for a given propeller diameter (a maximum diameter of 5.3 m is chosen limited by the ground clearance) and thrust requirement, more shaft power is required resulting in a reduced efficiency. The chosen propeller design method according to Adkins and Liebeck [18] combines the momentum theory and the blade element

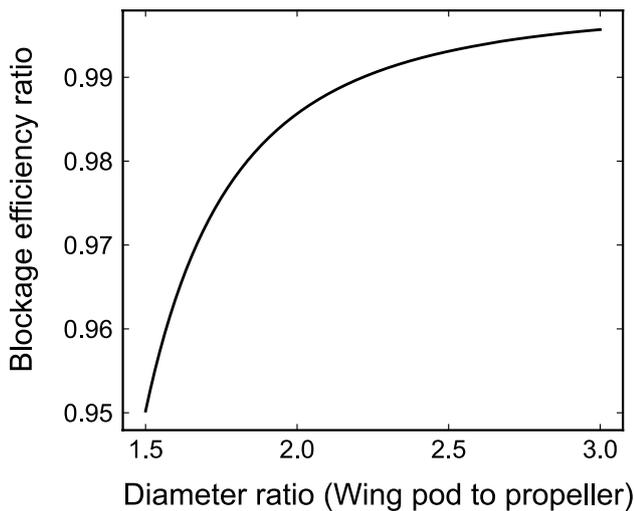**Fig. 6** Shape of wing pod fairing including the installation space

Fig. 7 Propeller efficiency loss due to blockage by the wing pod fairing downstream [15–18]

Fig. 8 Sketch of the liquid hydrogen storage, its control volumes, mass and energy flows

theory while considering the conditions for minimum energy loss. Figure 7 shows the efficiency ratio (efficiency of blocked propeller divided by efficiency of isolated propeller) depending on the diameter ratio (propeller diameter divided by spinner diameter). As can be seen, the diameter ratio should be higher than two to reduce the efficiency loss.

2.2.5 Thermodynamic analysis

To predict the ullage pressure, the heat and mass transfer of the liquid hydrogen storage tank, a dynamical model is carried out. The liquid hydrogen and vapor, as well as the tank structure and insulation layers are considered. The modeling approach is explained in the following section.

To describe the thermodynamic behavior of the hydrogen storage, a reduced lumped-parameter model based on [19] is used within this study. This model applies basic conservation laws for the mass and energy exchange processes of a rocket propellant loading with liquid hydrogen. Referring to Fig. 8, the control volumes (CV) for the adapted model in this study are shown.

It distinguishes between liquid (CV 1) and gaseous hydrogen (CV 2) separated by an interface in between the two phases (CV 3). The inner containment wall is split into two control volumes depending on the filling level: a CV adjacent to the vapor (CV 4) and one surrounding the liquid hydrogen (CV 5). In this sketch, the insulation layers are represented by a single CV (CV 6), but are composed of different layers depending on the insulation architecture. The skin layer (CV 7) envelopes the insulation layers and sets the system boundary to the ambient.
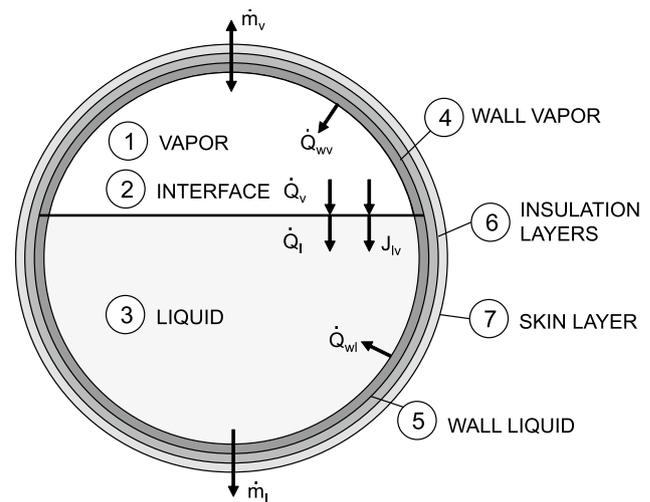
All control volumes exchange energy and/or mass. From the liquid control volume, LH2 is withdrawn and fed to the consumer, while the schedule of the mass flow depends on the thrust requirements of the flight mission. In addition, mass is exchanged at the interface, which will be described in detail at the next paragraph. Heat flux through the compartment wall is modeled by natural convection at the boundary between fluid and wall. Therefore, empirical equations for horizontal and vertical heat transfer coefficients are used, which are given for the lumped parameter approximation in appendix B of [20]. Since the heat transfer coefficients depend on the tank geometry, the shape of the storage compartment is simplified as a cylinder with same radius and volume to apply the empirical equations. Unlike reference [19], the temperature of the liquid is time-dependent and its density depends on the temperature. For the calculation of the thermodynamic properties of the liquid, like density, saturation pressure and saturation temperature, an open-source application [21] is used.

A very thin and massless film is introduced separating the vapor from the liquid hydrogen. The film is considered to be in saturated condition. Its temperature is assumed to be uniform and therefore is related to the vapor pressure [19, 20, 22]. Considering these assumptions, the energy balance equation for the film can be derived

$$\dot{Q}_v - \dot{Q}_l + J_{lv}(h_{evap}) = \frac{\mathrm{d}(m_{lv}u_{lv})}{\mathrm{d}t} = 0 \qquad (3)$$

where the mass flow for evaporation or condensation J_{lv} results in the balance of heat transfer at the interface. The heat flux is denoted as $\dot{Q}_{v(l)}$ and h_{evap} represents the enthalpy of evaporation. In contrast to [19], the used model does not

account for different modes of interfacial heat exchange, but is assumed to be dominated by natural convection at the interface as discussed by [22] and correlations for horizontal heat transfer coefficients are applied [20].

The vapor phase is modeled as an ideal gas [19] with time-dependent temperature and density. Since no helium is applied for pressurization, GH2 is the only gas present in the ullage volume. The mass flows crossing the boundaries are the evaporation or condensation mass flow at the interface. Also, the venting or pressurization mass flow crosses the control volume boundary when needed. For the energy balance, heat fluxes from the compartment wall and interface are considered, as well as the power due to compression (expansion) of the vapor. In addition, the transfer of energy resulting from the external mass flows and their corresponding enthalpy are included in energy balance. A detailed description of the mass and energy balances can be obtained from [19].

Besides the fluid, the storage compartment and insulation are included in the dynamical model. Each layer is considered a control volume having a heat capacity. In between the layers, heat is exchanged via conduction. The material properties of the insulation materials are temperature dependent and given in [4]. In case of multilayer insulation (MLI), a different approach is applied. In [23], the heat transfer of MLI is discussed for ideal and realized insulation systems showing a wide range of total heat flux. This heat flux can be divided into three parts: heat flux by radiation, gas conduction and solid conduction [23, 24]. The correct prediction of the heat flux depends on multiple factors and the application of the semi-empirical equation of [24] needs a calibration of a tested insulation system. Therefore, data from a calibrated multilayer insulation for a mobile liquid hydrogen tank is used [13] for this analysis and is implemented for a steady-state condition depending on the temperature difference. The requirements for the insulation of reference [13] are a vacuum pressure below 10^{-5} torr and equivalent heat flow of 5.9 W/m^2 for an outer vessel temperature of 298 K.

The heat exchange with the ambient at the skin layer is estimated by a method proposed in [25]. For the flight range below Mach 2 it is assumed, that the recovery temperature equals the skin temperature. Therefore, the skin temperature directly depends on the flight condition and the total temperature delta is determined by the difference between the temperature of the skin layer and the bulk temperature of LH2 or GH2, respectively. All correlations form a set of ordinary differential equations [19, 22]. This initial value problem is treated with the integrate library of the python package SciPy [26].

2.3 Integrated storage sizing

The sizing of the storage compartment is described in this section. The interdependencies, which are discussed qualitatively in Sect. 2, are transformed into an executable workflow within RCE [8] using CPACS [11] to connect the various tools. This methodology is analogous to the aircraft sizing procedure described in section 2.1. For the illustration and postprocessing, the parametric aircraft geometry modeler TiGL [27] is applied. Figure 9 represents the sizing workflow for the trade-off study.

Starting with a combination of design parameters and the aircraft data, the design loop is entered. Iteratively, the storage geometry is generated and the storage mass, aerodynamic drag and propeller blockage are calculated, as explained in Sects. 2.2.1, 2.2.2, 2.2.3, 2.2.4, the sensitivities regarding the design mission block fuel are estimated based on these effects and applied to the already calculated sensitivity data of Sect. 2.1.2. As a result, the block fuel for the design mission is adjusted and serves as an input for the dynamical simulation of the design mission. Within this simulation, the thermodynamic behavior of the liquid hydrogen storage is analyzed following the modeling approach in Sect. 2.2.5. At the end of the mission, the remaining liquid hydrogen, the vapor and the vented hydrogen are estimated. The ratio of block fuel to fuel reserves is compared to the design mission. This fuel ratio is taken as convergence criteria. If the reserves are underestimated (overestimated), the sizing fuel mass and the storage volume are increased (decreased). By the application of the convergence loop, the two feedback loops described in Sect. 2 can be addressed. This procedure is repeated for the given set of design parameters. The converged designs are discussed in the following section.

3 Results

This section deals with the results of the trade-off study. First, the design parameters are defined, then the different types of insulation are compared regarding the penalties on aircraft performance and fuel loss due to venting, as well as block fuel and dormancy time.

3.1 Parametric study

For the trade-off study, three aspects are identified as main design drivers: the storage geometry, the maximal pressure level and the insulation concept. As already discussed in Sect. 2, these parameters serve mostly as inputs for the coupled interactions and therefore are used as design parameters. To influence the geometry of the storage tank only the outer diameter of the cylindrical section is varied, while the
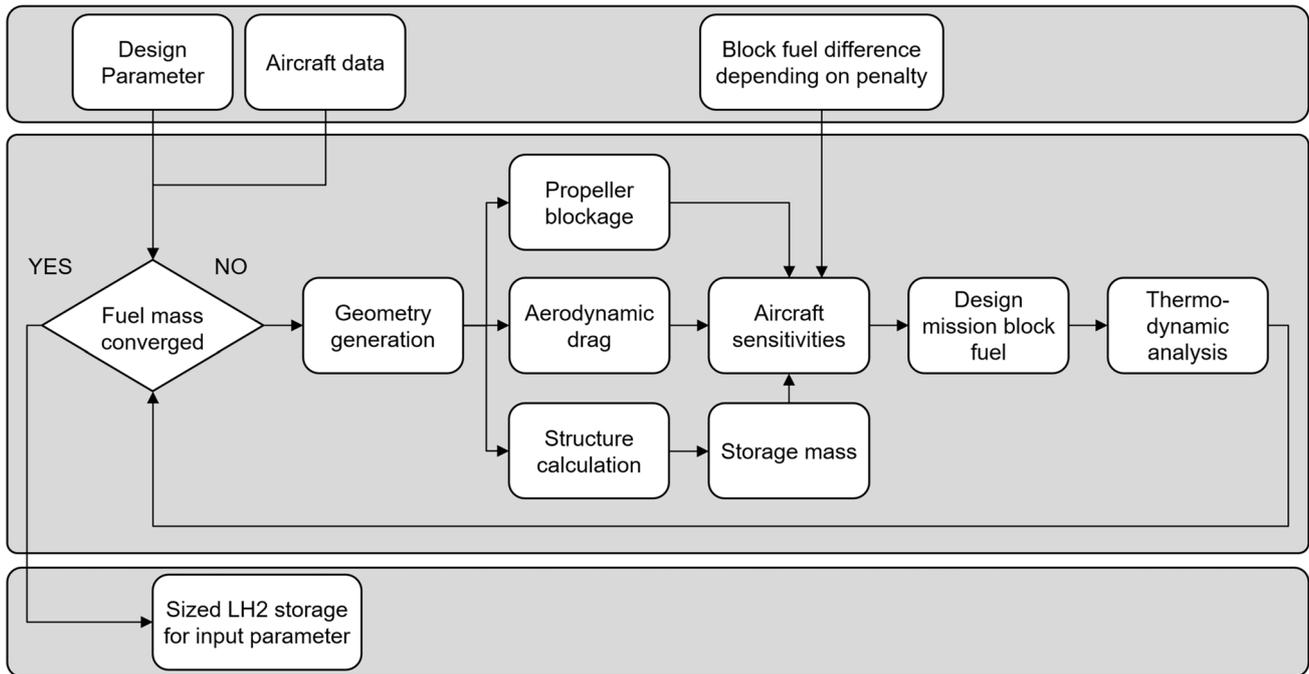
Fig. 9 Sizing workflow of the trade-off study

Table 2 Value range of design parameters

Parameter	Unit	Value range
Outer radius	m	0.9–1.4
Insulation type	–	Rigid foam/MLI
Variable foam thickness	m	0.02–0.1
Maximal pressure	Bar	1.5–3.0

generation of the shape follows predefined production rules. For instance, the ratio of storage diameter and conical section is fixed to 2 and the shape of the tank dome is related to the torispherical dome given in [4]. The second parameter is the maximal pressure level, where 3.0 bar sets the upper bound. The third parameter is the insulation concept. Two types of insulation are applied: multilayer insulation and rigid foam insulation. For the latter, the insulation thickness is also varied affecting not only the insulation efficiency, but also the shape and mass of the storage tank. In Table 2, the value ranges of the design parameters are listed.

3.2 Design mission

The sizing of the storage compartment is based on the design mission. The range of the design mission is 1500 nm and the cruise Mach number of 0.62. For the 250 passengers, a payload of 23.75 tons is assumed. The time-dependent altitude and fuel flow per tank are illustrated in Fig. 10. The fuel flow depends on the aircraft performance and is shown exemplary
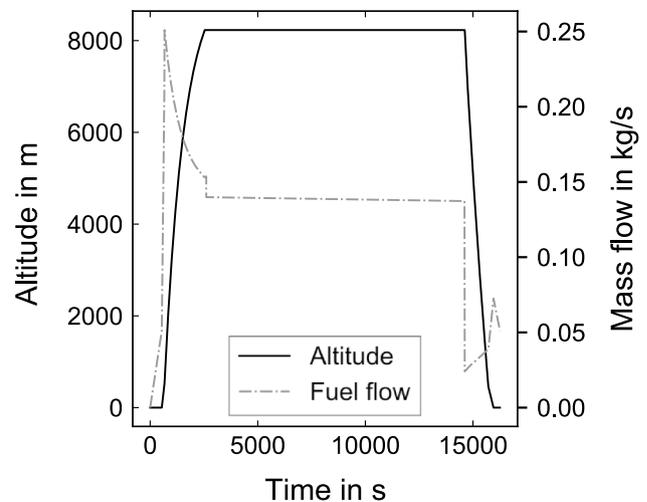

Fig. 10 Time-dependent altitude and fuel flow for the design mission

for an insulation based on rigid foam with a variable insulation thickness of 6 cm and a maximal pressure of 2.0 bar.

In Figs. 11 and 12, temperature variation of the hydrogen control volumes (CV 1–3) and pressure variation for the exemplary design mission are presented. Initially, the vapor and liquid are set at 21.5 K, corresponding to a saturation pressure of about 1.5 bar. The temperature distribution of the insulation layers is calculated at steady state on ground before the mission is simulated. At this point, the liquid volume fraction is 95 %. Typical values of initial
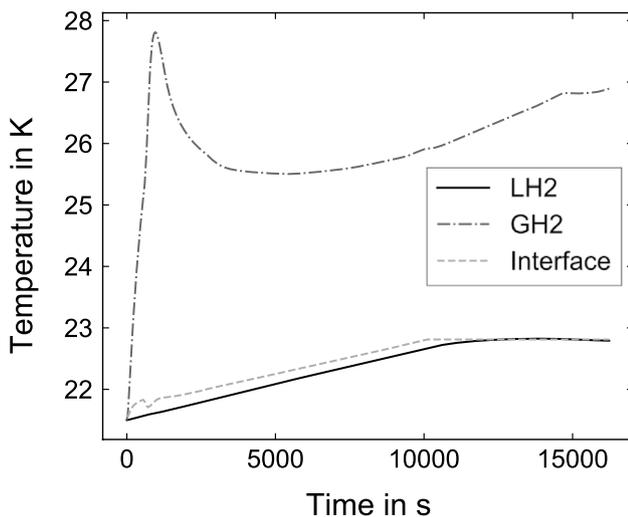
Fig. 11 Exemplary temperature variation of LH2, GH2 and the interface film for the design mission
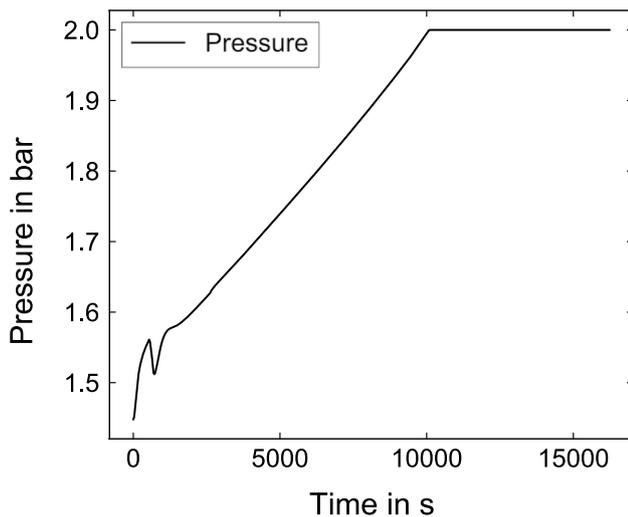

Fig. 12 Exemplary pressure variation for the design mission

ullage volume for propellant tanks for space applications are in the range of 3–10 % [28].

During the mission the temperature of the liquid increases up to the point, where the maximal operating pressure is reached and venting must be applied. After this state, the heat flux entering the storage tank directly leads to an increase of boil-off since saturated conditions are reached. The pressure and temperature variation of the vapor are coupled by the ideal gas assumption. At the point of maximal fuel flow, pressure drops due to the expansion of the vapor. The pressure gradient is determined by the heat transfer into the vapor and the change of its volume. Increasing (decreasing) the insulation quality, the pressure gradient decreases (increases). In addition, increasing the

maximal operating pressure venting has to be applied at a later point in time.

3.3 Rigid foam insulation

The results of the parameter study of the rigid foam insulation are discussed in the following sections. In Sect. 3.3.1, the effects on the aircraft performance and fuel loss due to venting are described. Based on that, the total block fuel for the sized storage compartments is compared in Sect. 3.3.2.

3.3.1 Aircraft performance and hydrogen venting

The effects imposed by the design parameters can be interpreted as fuel penalties. Two competing phenomena are identified: the indirect effect on the aircraft performance and the fuel loss of vented hydrogen. In Fig. 13, the performance penalty and the vented hydrogen are shown.

In the left column of Fig. 13, the combined effects of the storage mass, the aerodynamic drag and propeller blockage are shown. For each pressure level, the variation of outer radius and variable insulation thickness are displayed. The distribution of the contours is similar for each pressure level. A minimal influence on the aircraft performance exists for a radius in between 1.0 and 1.2 m and for the minimal insulation thickness. In contrast to that, for a thick insulation and big radii, the aircraft performance is penalized the most. The fuel penalty increases with increasing maximal pressure level. To understand the contour, the effects are described separately.

The calculation of the storage compartment mass shows different dependencies. The weight of the insulation layers scales with the surface of the storage tank and the insulation thickness. The biggest fraction of the weight of all layers takes the inner structural aluminum layer. Here, the trend points into diverging directions. Like the insulation, the mass scales with the surface area, but the thickness of the aluminum wall depends on the radius and the pressure level, respectively. For example, the minimal wall thickness at 0.9 m radius and max. pressure of 1.5 bar equals to 1.7 mm following the calculation approach of Sect. 2.2.2, while the maximal wall thickness is 4.5 mm at 1.4 m radius and 3.0 bar max. pressure.

The propeller blockage only depends on the outer pod diameter. For the maximal diameter of 2.8 m, the propulsive efficiency loss caused by propeller blocking is estimated to 1.77 % and for the minimal diameter to 0.45 %, respectively. Since the influence is not linear on the pod diameter, especially bigger diameters are penalized and therefore this restraint sets a boundary for the integration as wing pods.

The aerodynamic drag depends primarily on the outer radius since this parameter defines mostly the shape of the wing pod. In addition, the sizing volume and the insulation
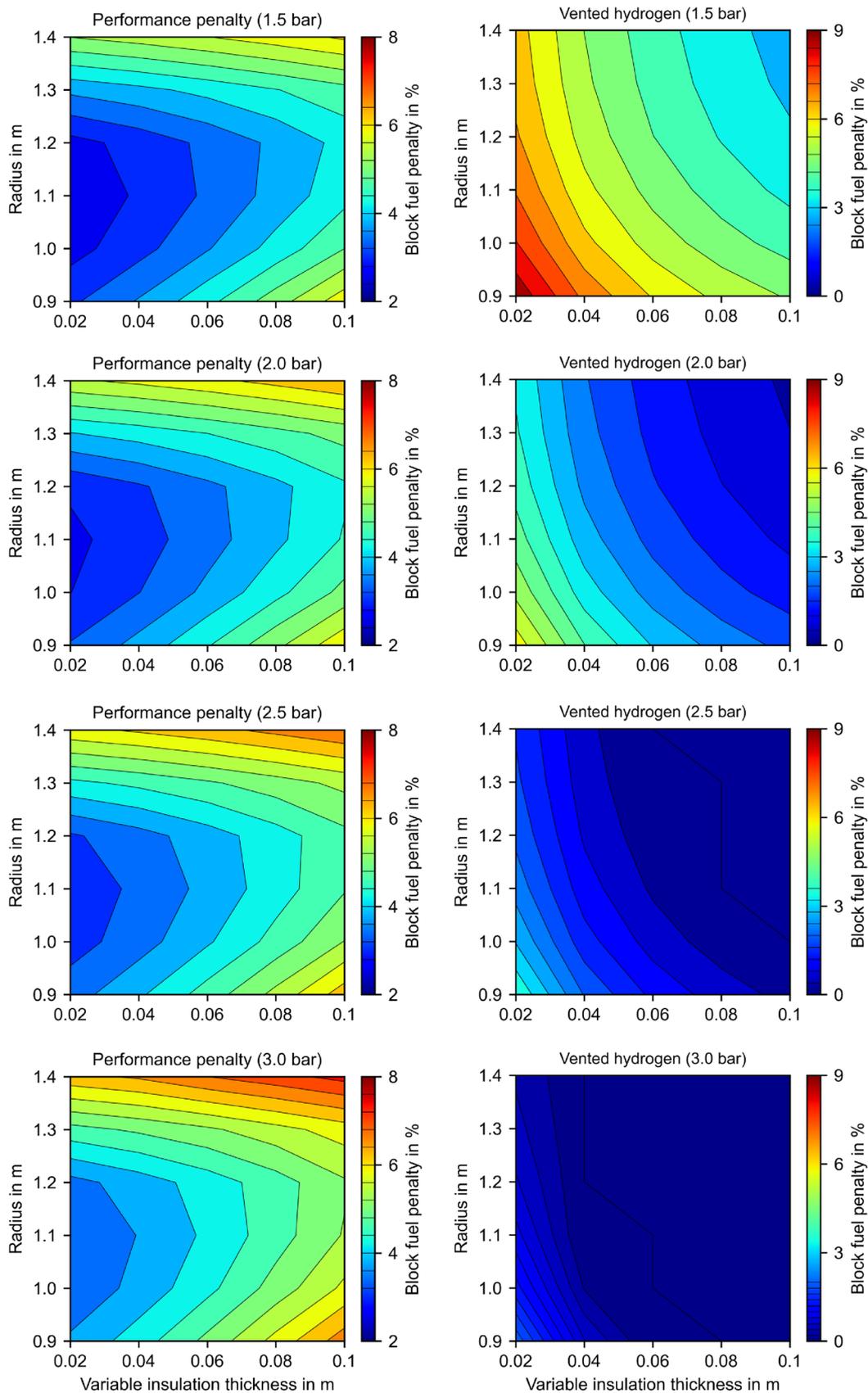
Fig. 13 Block fuel penalties (rigid foam insulation) due to aircraft performance (left) and fuel loss by venting (right) in % compared to fixed initial assumptions

thickness impact the shape. The minimal aerodynamic drag is obtained for a radius of 1.2 m and a minimal insulation thickness, and equals to 2154 N per pod. For smaller and bigger radii, the drag increases: bigger radii lead to disproportionate drag increase and for smaller radii the influence of the increased wetted area (the shape gets thinner and longer) predominates the aerodynamic drag. These effects in combination with the sizing volume lead to the contours presented on the left column and represent the first feedback loop.

On the right side of Fig. 13, the effect of the second feedback loop is displayed: the fuel loss due to hydrogen venting. The fuel loss due to hydrogen venting is obtained from the thermodynamic mission simulation. As explained in the previous section, the point in time when venting is applied depends on the total heat flux entering the storage compartment, as well as the allowable pressure. Moreover, the total heat flux determines the mass flow of vented hydrogen.

Again, the fuel loss due to venting is expressed in percentage with respect to initial assumptions. Similar to the penalties on aircraft level, the contours are shown for a variation of radius and insulation thickness. The different pressure levels are addressed for each plot. Three trends can be observed considering the fuel loss due to venting. The first trend deals with the insulation quality. Increasing insulation thickness minimizes the heat flux per area.

Second, a high volume to surface ratio is favorable concerning the total heat flux. Therefore, the solutions with the biggest radius suffer the least fuel loss to venting. Especially for smaller radii and thick insulation, the generation of shape has an effect on the vented hydrogen. Since the outer radius is fixed as an input, with increasing insulation thickness, the inner radius of the hydrogen containment decreases. For a given sizing volume, the cylindrical part of the shape has to be stretched and this ultimately results in a low volume to surface ratio.

The last trend, which can be observed, relates to the maximal pressure determining the time-dependent start of hydrogen venting. While for a maximal pressure of 1.5 bar venting is applied from the start, none of the hydrogen vapor has to be vented during the mission for a variable insulation thickness greater than 6 cm and 3.0 bar maximal pressure. An additional increase of the maximal pressure does not result in less venting during the design mission. Summarizing the trends, the thermodynamic objectives are contrary to the penalties on aircraft level.

3.3.2 Design mission block fuel

The design mission block fuel is a key indicator of the trade-off study. Since the penalties on aircraft performance and fuel loss due to hydrogen venting follow opposing trends, the design mission block fuel combines the two feedback loops.
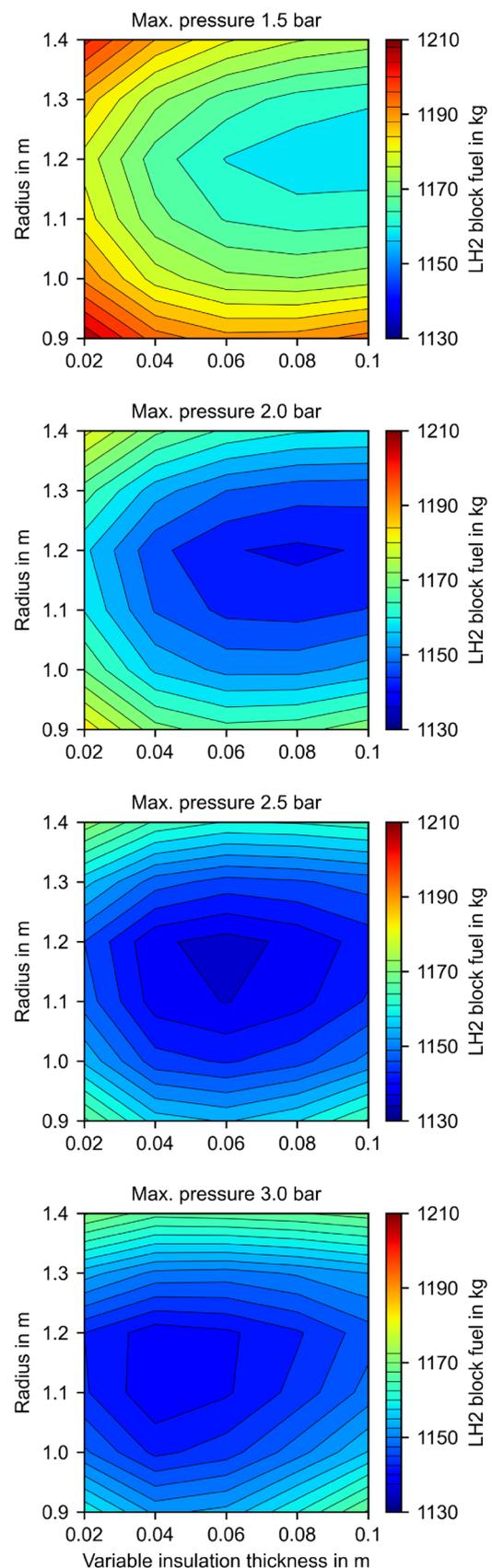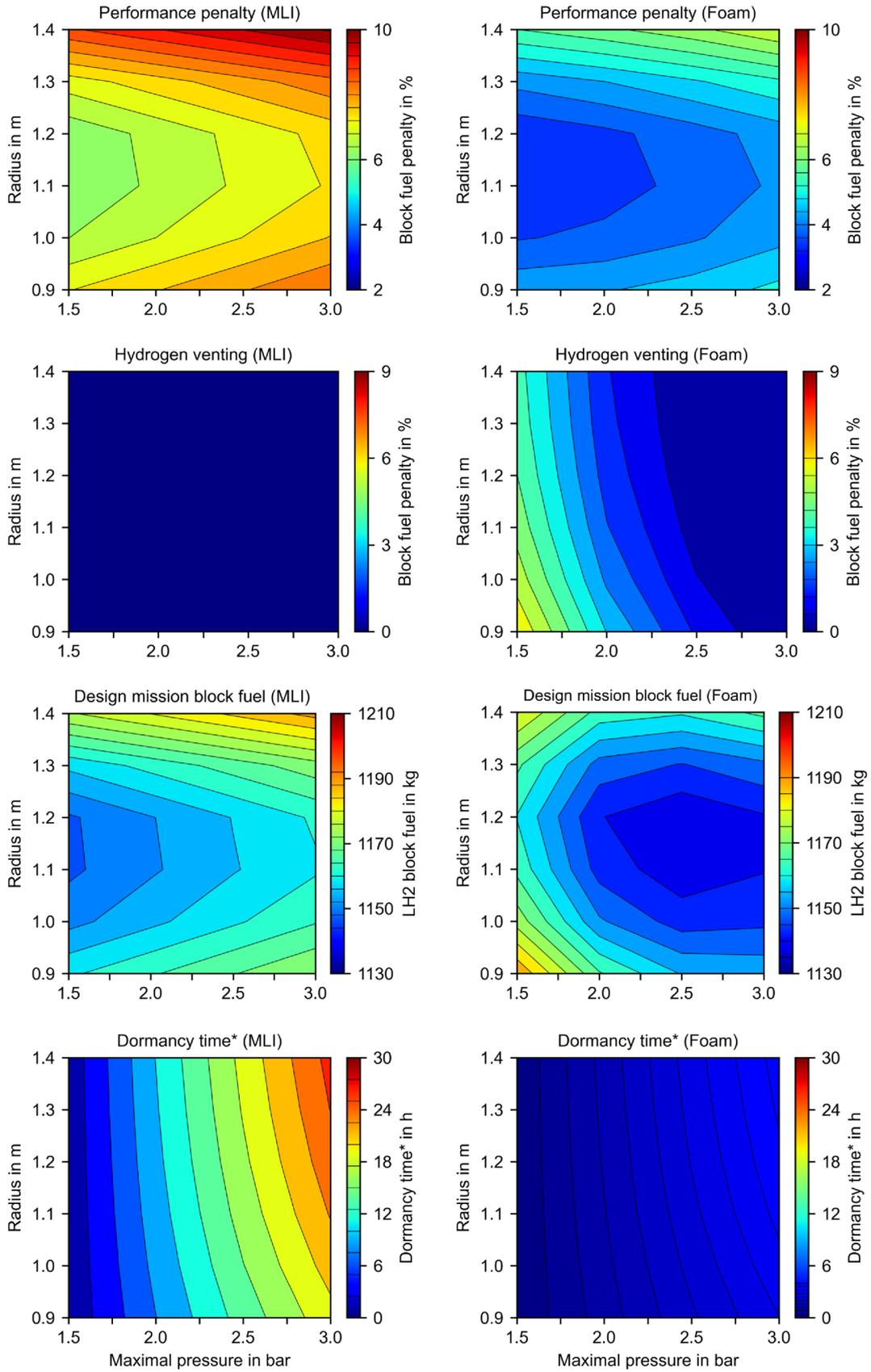

Fig. 14 Block fuel variation of rigid foam insulation

In Fig. 14, the variation of design mission block fuel per storage tank considering the rigid foam insulation is illustrated. Each maximal pressure level is represented by a plot. The block fuel varies depending on the outer radius and the insulation thickness.

For the lowest maximal pressure level of 1.5 bar, hydrogen venting dominates the design trade. A minimal block fuel is obtained for a thick insulation and a relatively big radius of about 1.2 m, stressing the importance of insulation quality if a low pressure level is applied. At a maximal pressure level of 2.0 bar, a significant decrease of the design mission block fuel is reached compared to the lowest pressure level. Since the penalties on aircraft level only slightly increase, the main difference is implied by the reduction of hydrogen venting, which is in the range of 3 % ref. block fuel. The optimal insulation thickness shifts to a variable insulation thickness of 8 cm at an outer radius of 1.2 m. Setting the maximal pressure level to 2.5 bar the optimal parameter range shifts toward 6 cm variable insulation thickness, where the global minimum of design mission block fuel is obtained. For the aircraft, the minimal block fuel is estimated to 2271.6 kg (1135.8 kg per storage compartment). An additional increase of the maximal pressure level does not result in a further decrease of block fuel. Hydrogen venting is only reduced for storage compartments with thin insulation and small radius, and the increase in storage mass is applied to all designs.

3.4 Multilayer insulation

The design trades of the multilayer insulation depend on the storage compartment shape and the maximal pressure level. A variation of the insulation quality (e.g., a variation of the vacuum pressure or the number and density of heat shields) was beyond the scope of this study. A comparison of rigid foam insulation and multilayer insulation is illustrated in Fig. 15, where, in the left column, MLI and, in the right column, rigid foam at a variable insulation thickness of 6 cm are shown. Four different aspects are compared to each other: the penalties on aircraft performance and due to hydrogen venting, the design mission block fuel and the dormancy time.

Comparing the penalties on aircraft performance, the multilayer insulation has an increased influence. Due to a higher mass of the double-walled storage structure and additional systems like the vacuum system, the storage mass is increased by a factor in the range of 1.8–2.1 depending on the design parameters. Therefore, the penalty in percent

block fuel is 3 % higher on average. The aerodynamic drag and propeller blockage are only slightly affected, since the shape is comparable for the chosen insulation thickness.

Since the total heat flux is drastically decreased by the application of multilayer insulation, no hydrogen must be vented during the design mission. For every flight phase, the pressure is maintained above the initial pressure by external evaporation of liquid hydrogen. In contrast to rigid foam insulation, the feedback loop regarding fuel loss due to venting is avoided for the storage sizing.

Considering the design mission block fuel, the contours of multilayer insulation are similar to the contours of the penalties on the aircraft performance, as there is no balancing between hydrogen venting and decreasing aircraft performance. The minimum design mission block fuel of multilayer insulation is estimated at the boundary of the parameter space at minimal pressure level and in between 1.1 and 1.2 m radius. Comparing the minimal design mission of the two insulation concepts, the optimal rigid foam concept performs about 1 % better in terms of block fuel with regard to the assumptions of this study.

Another aspect of the comparison is the dormancy time. The dormancy time depends on the initial and boundary conditions and the insulation quality. Since the initial and boundary conditions might vary for every mission, for the comparison of the insulation quality the initial conditions are set to a liquid temperature of 21.5 K at saturation pressure and a filling ratio of 50 %. The ambient temperature is set to international standard atmosphere (ISA) conditions on ground, while solar heat gain is neglected. The shapes of the contour of both insulation concepts have a similar appearance: With higher pressure the dormancy time is expanded. In addition, the total heat flux is influenced only by the ratio of volume to surface since the heat flux per area is identical for each insulation concept. A significant offset between the multilayer insulation and the concept based on rigid foam can be observed. Even for a maximal pressure level of 2.0 bar, MLI outperforms every parameter combination of rigid foam insulation. This shows the advantage of MLI for ground handling and operation.

4 Summary and conclusion

For the integration of a liquid hydrogen storage compartment in wing pods, a trade-off study was conducted. A short-range turboprop aircraft concept serves as a use-case and its sensitivities regarding mass, aerodynamic drag and propeller blockage are used to estimate the influence of the storage integration on the aircraft performance. To model these effects, conceptual and preliminary design methods are applied. A dynamical model for the thermodynamic behavior of the liquid hydrogen storage is used

enabling mission simulations. The effects of the integration approach are coupled making an integrated sizing of the storage compartment necessary. Two feedback loops are identified and interpreted as penalties on aircraft performance and penalties due to hydrogen venting, respectively. These opposing trends can be influenced by the design parameter of the trade-off study. The storage tank diameter, the insulation type and thickness, and the maximal ullage pressure level are chosen as parameters and span the design space. For the combination of these design parameters, the liquid hydrogen storage compartment is sized for the design mission of the aircraft concept.

The sizing of the insulation concept based on rigid foam is driven by the balance between fuel loss due to hydrogen venting and the influence of the wing pods on the aircraft performance. An optimal parameter combination is found at 1.2 m outer radius, a variable insulation thickness of 6 cm (resulting in an overall insulation thickness of about 11 cm) and a maximal pressure level of 2.5 bar. In contrast to the rigid foam insulation concept, the sizing of the multilayer insulation is influenced by the aircraft performance only, since the high insulation quality avoids venting during the design mission. This advantage is combined with an increase of the storage mass leading to a higher influence on the aircraft performance. The optimal parameter combination for the multilayer insulation concept regarding the design mission block fuel is an outer radius in between 1.1 and 1.2 m and the minimal pressure level. Comparing the optimal designs, the rigid foam concept performs 1 % better in terms of block fuel on the design mission. Considering the dormancy time, multilayer insulation outperforms the insulation concept based on rigid foam. The findings of the design study show design trends rather than optimal solutions.

Within this study, not all aspects of the integration and the comparison of the insulation concepts could be included. For instance, the material choices for the rigid foam insulation and the reliability of the vacuum insulation of MLI and its implications to failure may influence the design decisions. Moreover, the interaction of the fuel delivery system with the hydrogen storage on the one side and the consumer on the other might impose further requirements. The fuel system architecture also creates possibilities to utilize excessive gaseous hydrogen, which was regarded as loss within this study. In addition, future work could include advanced modeling techniques, like temperature stratification of the hydrogen storage to improve the prediction of the ullage pressure [20]. Also, more advanced structural methods for each storage tank sections and different material selections are of interest. As a concluding remark, it can be stressed that the required thermodynamic performance of the storage tank influences strongly the overall aircraft design. Considering this influence, the definition of the thermodynamic

requirements has to be chosen carefully and remains a challenge for the application of cryogenic hydrogen in the aviation sector.

Declarations

References

1. Flightpath 2050: Europe's Vision for Aviation. Policy / European Commission. Publ. Off. of the Europ. Union, Luxembourg (2011)
2. Airbus Deutschland GmbH: Liquid hydrogen fueled aircraft - system analysis: Final technical report: Cryoplane (2003)
3. D. Silberhorn, G. Atanasov, J-N. Walther, T. Zill: Assessment of hydrogen fuel tank integration at aircraft level. German Aerospace Congress (2019)
4. Brewer, G.D.: Hydrogen Aircraft Technology. CRC Press, Boca Raton (1991). http://www.loc.gov/catdir/enhancements/fy0731/90047972-d.html
5. Verstraete, D.: The potential of liquid hydrogen for long range aircraft propulsion (2009). https://dspace.lib.cranfield.ac.uk/handle/1826/4089
6. Sefain, M.J.: Hydrogen aircraft concepts and ground support (2005). https://dspace.lib.cranfield.ac.uk/handle/1826/2998
7. Hartmann, J., Nagel, B.: Eliminating climate impact from aviation - a system level approach as applied in the framework of the dlr-internal project exact (exploration of electric aircraft concepts and technologies). German Aerospace Congress (2021)
8. Boden, B., Flink, J., Först, N., Mischke, R., Schaffert, K., Weinert, A., Wohlan, A., Schreiber, A.: Rce: An integration environment for engineering and science. SoftwareX **15**, 100759 (2021). https://doi.org/10.1016/j.softx.2021.100759
9. Wöhler, S., Atanasov, G., Silberhorn, D., Fröhler, B., Zill, T.: Preliminary aircraft design within a multidisciplinary and multifidelity design environment. Aerospace Europe Conference 2020 (2020)
10. Fröhler, B., Hesse, C., Atanasov, G., Wassink, P.: Disciplinary Sub-Processes to Assess Low-Speed Performance and Noise Characteristics within an Aircraft Design Environment. Deutsche Gesellschaft für Luft- und Raumfahrt - Lilienthal-Oberth e.V (2021). https://doi.org/10.25967/530201

11. Alder, M., Moerland, E., Jepsen, J., Nagel, B.: Recent advances in establishing a common language for aircraft design with cpacs. Aerospace Europe Conference 2020 (2020)

12. Zamboni, J., Zamfir, A., Moerland, E.: Semantic knowledge-based-engineering: The codex framework. In: Proceedings of the 12th International Joint Conference on Knowledge Discovery, Knowledge Engineering and Knowledge Management, pp. 242–249. SCITEPRESS - Science and Technology Publications, Web based (2020). https://doi.org/10.5220/0010143202420249

13. Stroman, R.O., Schuette, M.W., Swider-Lyons, K., Rodgers, J.A., Edwards, D.J.: Liquid hydrogen fuel system design and demonstration in a small long endurance air vehicle. Int. J. Hydrogen Energy **39**(21), 11279–11290 (2014). https://doi.org/10.1016/j.ijhydene.2014.05.065

14. AD 2000-Regelwerk: Taschenbuch-Ausgabe 2016, 10. auflage edn. Handbuch Technische Regeln. Beuth Verlag GmbH, Berlin (2017)

15. Torenbeek, E.: Synthesis of Subsonic Airplane Design: An Introd. to the Preliminary Design of Subsonic General Aviation and Transport Aircraft, with Emphasis on Layout, Aerodynamic Design, Propulsion and Performance. Univ. Pr, Delft (1982)

16. Schlichting, H., Truckenbrodt, E.: Aerodynamik des Flugzeuges: Erster Band: Grundlagen aus der Strömungstechnik Aerodynamik des Tragflügels (Teil I), 3. auflage edn. Klassiker der Technik. Springer, Berlin and Heidelberg (2001). https://doi.org/10.1007/978-3-642-56911-1

17. Raymer, D.P.: Aircraft Design: A Conceptual Approach, Sixth edition edn. AIAA education series. American Institute of Aeronautics and Astronautics Inc, Reston, VA (2018)

18. Adkins, C.N., Liebeck, R.H.: Design of optimum propellers. J. Propul. Power **10**(5), 676–682 (1994). https://doi.org/10.2514/3.23779

19. Osipov, V.V., Daigle, M.J., Muratov, C.B., Foygel, M., Smelyanskiy, V.N., Watson, M.D.: Dynamical model of rocket propellant loading with liquid hydrogen. J. Spacecr. Rocket. **48**(6), 987–998 (2011). https://doi.org/10.2514/1.52587

20. Daigle, M.J., Smelyanskiy, V.N., Boschee, J., Foygel, M.: Temperature stratification in a cryogenic fuel tank. J. Thermophys. Heat Transfer **27**(1), 116–126 (2013). https://doi.org/10.2514/1.T3933

21. Goodwin, D.G., Speth, R.L., Moffat, H.K., Weber, B.W.: Cantera: An Object-oriented Software Toolkit for Chemical Kinetics, Thermodynamics, and Transport Processes. Zenodo (2021). https://doi.org/10.5281/ZENODO.4527812

22. Estey, P.N., Lewis, D.H., Connor, M.: Prediction of a propellant tank pressure history using state space methods. J. Spacecr. Rocket. **20**(1), 49–54 (1983). https://doi.org/10.2514/3.28355

23. VDI-Wärmeatlas: Mit 320 Tabellen, 11., bearb. und erw. aufl. edn. Springer Reference. Springer Vieweg, Berlin (2013)

24. Hedayat, A.: Analytical modeling of variable density multilayer insulation for cryogenic storage. In: AIP Conference Proceedings, pp. 1557– 1564. AIP, Madison, Wisconsin (USA) (2001). https://doi.org/10.1063/1.1472190

25. AC-9 Aircraft Environmental Systems Committee: SAE Aerospace Applied Thermodynamics Manual Aerothermodynamic Systems Engineering and Design. SAE International, 400 Commonwealth Drive, Warrendale, PA, United States (2011). https://doi.org/10.4271/AIR1168/3A

26. SciPy Community: SciPy Documentation. https://docs.scipy.org/doc/scipy/reference/generated/scipy.integrate.odeint.html Accessed 17 Aug 2021

27. Siggel, M., Kleinert, J., Stollenwerk, T., Maierl, R.: Tigl: An open source computational geometry library for parametric aircraft design. Math. Comput. Sci. **13**(3), 367–389 (2019). https://doi.org/10.1007/s11786-019-00401-y

28. Sutton, G., Biblarz, O.: Rocket Propulsion Elements, 9th edn. Wiley, New York, NY (2017)